Short Papers

Analysis of GNSS Performance Index Using Feature Points of Sky-View Image

Woonki Hong, Kwangsik Choi, Eunsung Lee, Sunghyuck Im, and Moonbeom Heo

***Abstract*—When sky-view factor (SVF) is used to predict the positioning performance of the global navigation satellite system (GNSS), it is easy to use the SVF as a performance index without a specific database, as it is used for topographic maps, not only in an open-sky land but also in regions where there are many tall buildings. However, conventional SVF is only able to express the degree of openness of the sky as a ratio, and it is limited to being used as a performance index for the positioning that uses the GNSS. When the conventional SVF is used in a land transportation environment, the predicted value for the positioning performance of the GNSS is often not consistent with the actual positioning error, but when sky-view-based dilution of precision (SVDOP) is applied, we confirmed that it was substantially close to the actual positioning error. This confirms our expectation that the utilization of the proposed method rather than the utilization of SVF alone in land transportation environments will make the analysis easier. In this paper, the SVDOP is calculated with real Global Positioning System data, and its usefulness is validated by comparing it with the conventional SVF and the DOP.**

***Index Terms*—Global navigation satellite system (GNSS) dilution of precision (DOP), land road environment, performance, sky-view factor (SVF).**

I. Introduction

Errors in positioning when positioning is carried out using a global navigation satellite system (GNSS) signal are affected by performance indexes such as satellite visibility, dilution of precision (DOP), and the signal-to-noise ratio. In general, before positioning is carried out when a GNSS signal is used in surveying, the performance indexes for the relevant land region are analyzed [1], and surveying in that region is carried out at a time when the predicted error value of the GNSS is lowest.

Such performance indexes are widely utilized in regions where satellite visibility is favorable, such as open sky environments. Utilization is less common when a large number of tall buildings are distributed in the surroundings, as is the case in land transportation environments. In the case in which a region is not open sky, a 3-D topographic map of the surroundings of the survey point is needed [2], which is used to carry out the performance analyses. It is difficult, however, to obtain a 3-D topographic map of the relevant region, and although such a map is acquired, it takes a considerable amount of time to develop a program to use the map to predict the performance indexes in a specific region.

To address this problem, this paper proposes a sky-view-based DOP (SVDOP) as a performance index that can be widely used when positioning is carried out using a GNSS signal in a land transportation environment. The SVDOP, which was developed by applying sky-view factor (SVF), is able to overcome the conventional problems of the SVF.

To obtain sky-view images, a fish-eye lens with a 180° angle of view was used to capture images, and the captured images were passed through an edge-detection filter to obtain edge images, which were then binarized to obtain sky-view images. Twelve virtual lines were drawn at 30° intervals radiating from the center of the sky-view images thus obtained, and the points where the virtual lines intersect with the sky-view image were selected as the singularity points, which were then used to calculate the DOP.

When conventional SVF is used in a land transportation environment, the predicted value for the positioning performance of the GNSS is often not consistent with the actual positioning error, but when the SVDOP is applied, we confirmed that it was substantially close to the actual positioning error. This confirms our expectation that the utilization of the proposed method rather than the utilization of SVF alone in land transportation environments will make the analysis easier.

II. SVF

The SVF is a parameter that indicates the extent to which the sky can be observed from a given position on a road. When the sky is entirely visible, as is the case in an open-sky land, the SVF is 0. When the sky is entirely blocked off, as is the case in densely enclosed regions, the SVF is 1. In general, there are three methods to calculate the SVF. The first method makes use of geometrical conditions and the second method uses imaging science [3]. The third method uses the GNSS.

The geometric method is a method of simple modeling that was developed in the 1980s, which takes into consideration the ratio of the height and width of city center buildings. Current research, however, prefers the method based on imaging science because it theoretically produces more accurate results.

The optical imaging method uses a fish-eye lens to capture the environment 360° around the position that is to be measured, and this method is able to find the SVF value through image processing [4].

Recently, the calculation time of the SVF decreases because the digital camera/fish-eye lens is used [5] (see Fig. 1 for a photo captured by a fish-eye lens). The methods of digital image processing improve the efficiency of the SVF calculation [6]. To produce the SVF, occasionally, a 3-D geographic information system map is used [2].

The method for using the GNSS to calculate the SVF involves calculating the coordinates of the GNSS that can be observed from a specific location, predicting the DOP and converting it to the SVF. This method is relatively easy to implement, but a drawback is that it is about 20% less accurate than the method that uses a fish-eye lens [7].

Manuscript received January 29, 2013; revised June 1, 2013 and August 23, 2013; accepted September 4, 2013. Date of publication October 25, 2013; date of current version March 28, 2014. This work was supported by the Ministry of Land, Transport, and Maritime Affairs through the development of the global-navigation-satellite-system-based transportation infrastructure technology (06 Transportation Research and Development Report A3). The Associate Editor for this paper was F. Zhu.

The authors are with the Korea Aerospace Research Institute, Daejon 305-806, Korea.

Color versions of one or more of the figures in this paper are available online at http://ieeexplore.ieee.org.

Digital Object Identifier 10.1109/TITS.2013.2282631

Fig. 1. Sky view captured by a fish-eye lens.

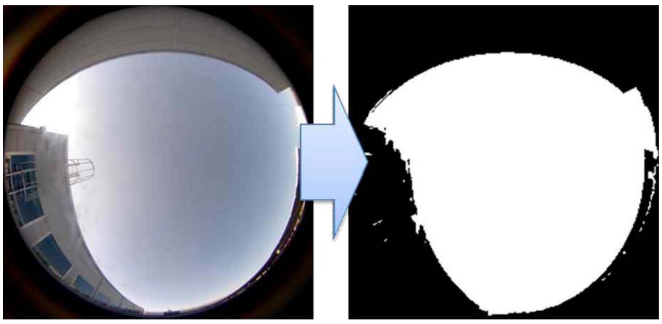

Fig. 2. SVF 0.31 configuration 1.

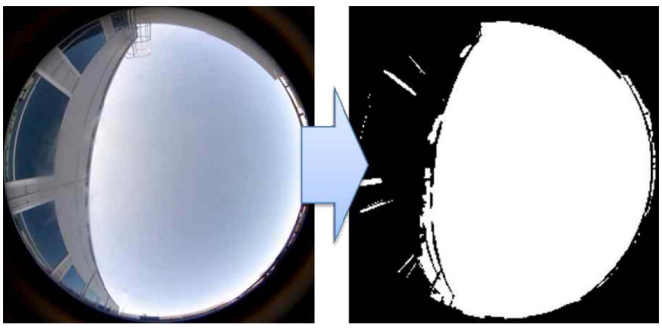

Fig. 3. SVF 0.31 configuration 2.

III. Problems of Applying GNSS to SVF

When the SVF is used to predict the positioning performance of the GNSS, it is easy to use the SVF as a performance index without a specific database, as it is used for topographic maps, not only in an open-sky land but also in regions where there are many tall buildings.

However, the conventional SVF is only able to express the degree of openness of the sky as a ratio, and it is limited to being used as a performance index for the positioning that uses the GNSS.

When the sky view of a specific region is to be observed, the SVF is 0.31 in both the cases in Figs. 2 and 3 [8]. (For the satellite geometry of configurations 1 and 2, see Fig. 4.)

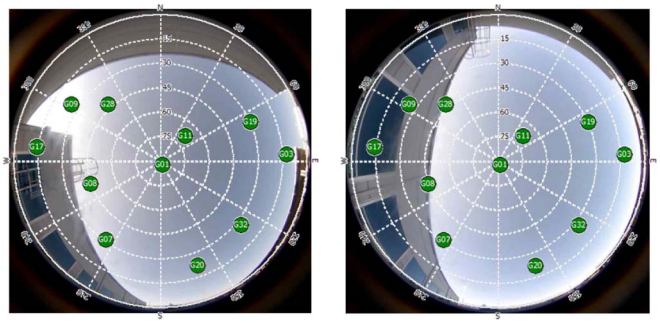

Fig. 4. Satellite geometry of configurations 1 and 2.

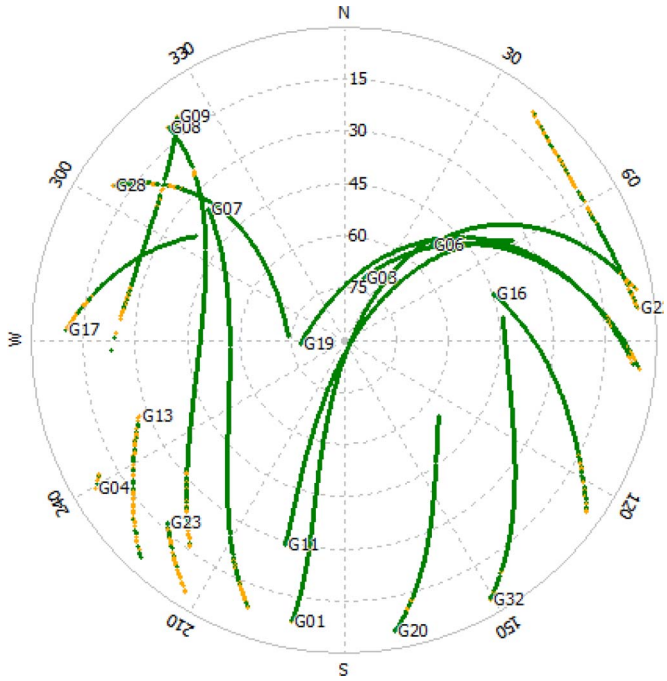

Fig. 5. Sky plot in configuration 1.

However, ten navigation satellites are observed in the left side of the figure, whereas seven satellites are observed in the right side of the figure, which indicates that they represent different situations.

Fig. 5 is the sky plot using real data in configuration 1, and Fig. 6 is the sky plot using real data in configuration 2. Figs. 5 and 6 show that configuration 1 has better signal quality than configuration 2.

Fig. 7 is the navigation result in configuration 1 and Fig. 8 is the navigation result in configuration 2.

For this reason, in a region where the surroundings include buildings, such as a land transportation environment, the SVF cannot be directly used as a performance index for the GNSS positioning.

IV. SVDOP

In order to resolve the problems that arise when the SVF is directly used as a performance index for the GNSS in a land transportation environment, this paper proposes a novel DOP based on a sky view. The novel DOP is named the SVDOP, and this section offers a step-by-step explanation of the method used to calculate the SVDOP [9].

The SVDOP is calculated by applying sky-view images. Images captured using a fish-eye lens with a 180° angle of view are binarized in order to obtain sky-view images and 12 virtual lines are drawn at 30° intervals radiating from the image center. The points where the

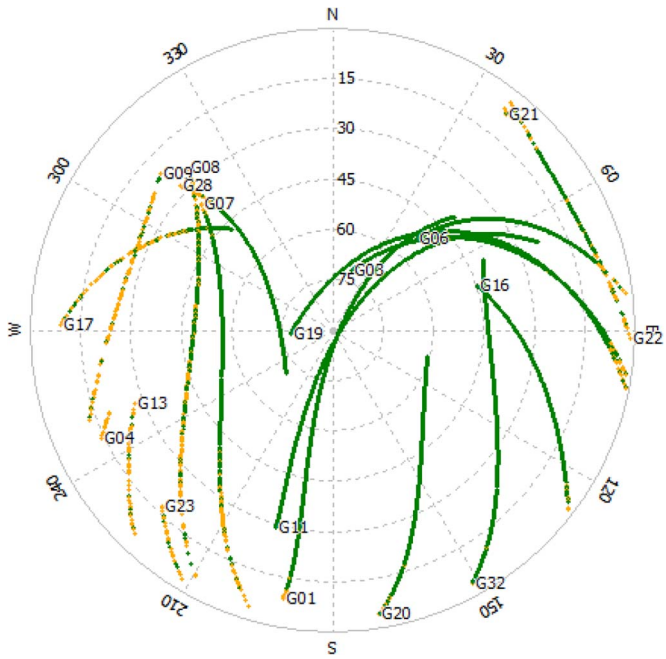

Fig. 6. Sky plot in configuration 2.

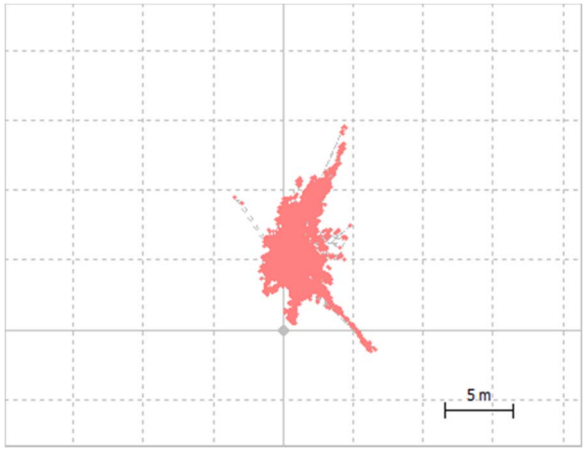

Fig. 7. Navigation result in configuration 1.

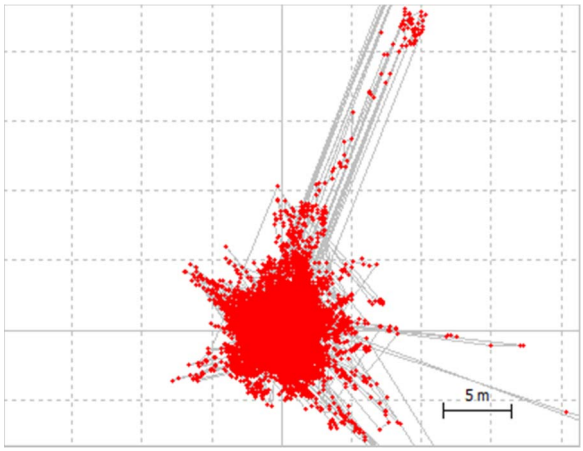

Fig. 8. Navigation result in configuration 2.

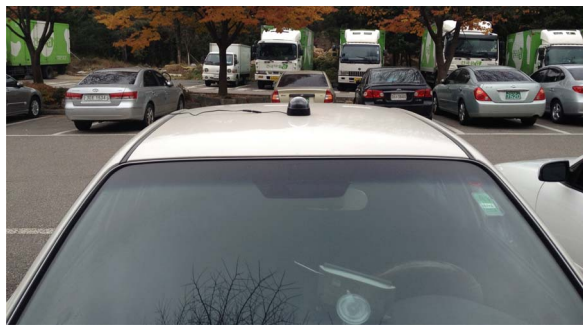

Fig. 9. Installation of the fish-eye lens.

Fig. 10. Captured sky-view image.

virtual lines and a sky-view image meet are selected as singularity points, and the position of the singularity points are converted to a Cartesian coordinate system. Then, this system is assumed to represent the virtual navigation satellite coordinates in order to calculate the horizontal DOP (HDOP). The DOP that is calculated in this manner is named the SVDOP. The SVDOP will be different depending on the observation environment as well as when the SVF value is the same, and it can be utilized as a performance index for the GNSS positioning.

A. Image Capturing

To obtain accurate sky-view images, images were captured by a camera that was positioned perpendicularly to the sky at the approximate center of the rooftop of a survey vehicle. The lens that was used was a fish-eye lens that is capable of capturing a 360° image.

The fish-eye lens was mounted onto the approximate center of the rooftop of a vehicle, as shown in Fig. 9. This enabled the user to capture sky-view images to predict the GNSS performance when quickly moving in a land transportation environment. The images captured in this manner are similar to that shown in Fig. 10.

B. Application of Edge-Detection Filter

To simplify the captured sky-view images and to define the specific regions in them, binarization is carried out, and an example of this is shown in Fig. 11 [10]. In order to binarize the sky-view images, the

Fig. 11. Binarized sky-view image.

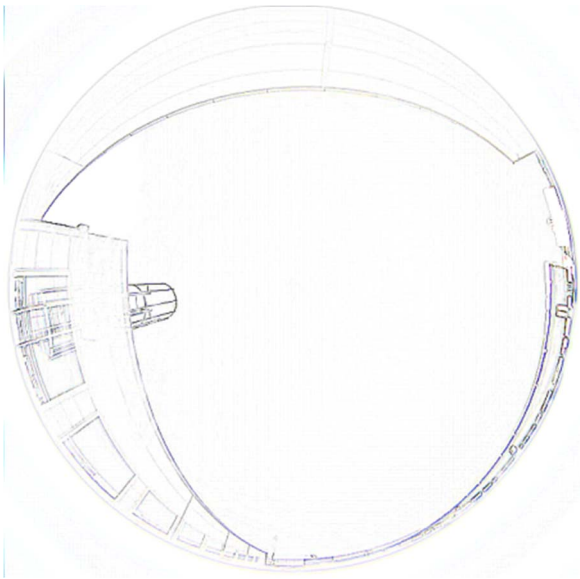

Fig. 12. Image made by edge filter.

binarization scale needs to be adjusted to match each image. When the scale is adjusted and binarization is implemented, it was confirmed that the region is showing that the building had disappeared, as shown in Fig. 11.

Rather than simply binarizing the sky-view images, it was considered preferable for the images to be first passed through an edge-detection filter in order to confirm the edge portions of buildings or barriers, after which binarization would be carried out. Fig. 12, presents a diagram in which the sky-view image that is captured in Fig. 10 has passed through an edge-detection filter in order to determine the edges in the image.

C. Calculation of Singularity Points

Following the detection of the edge portions of buildings or barriers, as shown in Fig. 12, arbitrary straight lines are drawn at 30° intervals radiating from the center, as shown in Fig. 13.

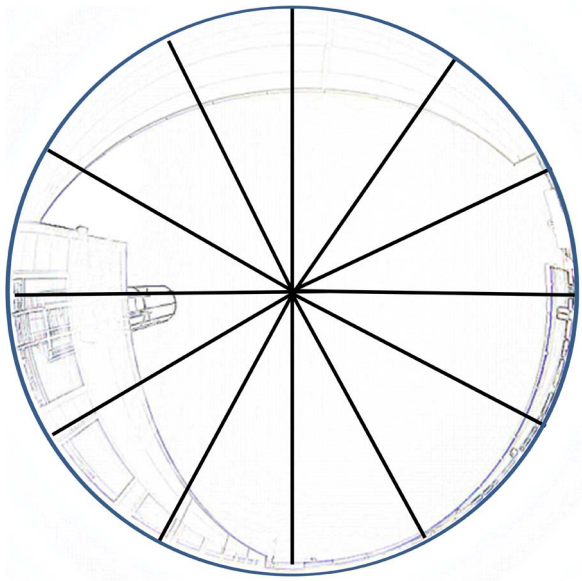

Fig. 13. Virtual straight lines at 30° intervals.

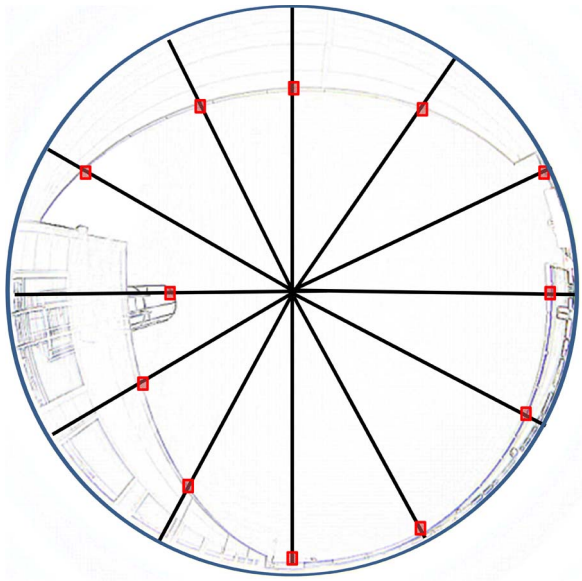

Fig. 14. Twelve singularity points.

When the arbitrary straight lines drawn at 30° intervals radiating from the center meet an edge region of the sky-view image that has gone through the edge-detection filter, the 12 points where the straight lines radiating from the center and the edge regions meet are selected as singularity points, as shown in Fig. 14.

D. Method for Calculating DOP

The types of DOP that are used as a positioning performance index that utilizes GNSS measurement values include the geometric DOP (GDOP), the HDOP, the vertical DOP, and the time DOP. The following is an explanation of the series of steps on how the DOP is calculated [11], [12].

A code measurement value for an ith navigation satellite can be developed, as shown in

$$\rho_u^i = \sqrt{(x_i - x_u)^2 + (y_i - y_u)^2 + (z_i - z_u)^2} + cb_u + v_i \quad (1)$$

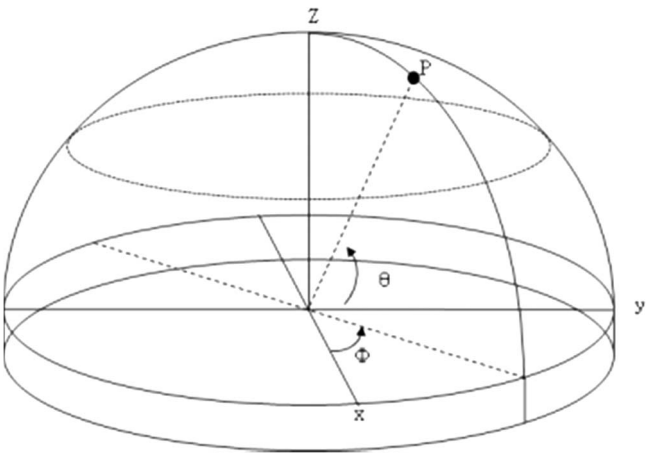

Fig. 15. Relationship between spherical coordinates and Cartesian coordinates.

where ρ is a GNSS code measurement value, i is a navigation satellite identifier, u is a user identifier, x_i, y_i, z_i denotes the coordinates of navigation satellite i, x_u, y_u, z_u denotes the coordinates of user u, c is the speed of light, b_u is the clock bias for a receiver, and v is the measurement noise.

When (1) is linearized for n satellites based on the initial user position x_o, y_o, z_o, the following can be derived:

$$\Delta\rho = H\Delta x + v \tag{2}$$

where Δ_ρ is a pseudodistance difference vector, H is the line-of-sight matrix of a navigation satellite for a linearization reference point, Δx is the vector of the receiver clock error and user coordinates relative to the linearization reference point, and v is a measurement noise vector.

Assuming an ith row of h_i for the matrix H in (2) gives

$$h_i = \left[-\frac{x^i - x_o}{\rho_o^i} - \frac{y^i - y_o}{\rho_o^i} - \frac{z^i - z_o}{\rho_o^i} \right]. \tag{3}$$

In this way, it can be confirmed that the physical meaning of matrix H is the line-of-sight vector for the observation satellite relative to the initial user position.

The GDOP is related to the matrix H in (2) and is calculated by applying a diagonal component of $(\overline{HH}^T)^{-1}$. When positioning is carried out in a land transportation environment, the horizontal plane error is a very important subject of interest; therefore, the HDOP is used as a performance index. A method to calculate the HDOP is explained as

$$(HH^T)^{-1} = \begin{bmatrix} D_{11} & D_{12} & D_{13} & D_{14} \\ D_{21} & D_{22} & D_{23} & D_{24} \\ D_{31} & D_{32} & D_{33} & D_{34} \\ D_{41} & D_{42} & D_{43} & D_{44} \end{bmatrix} \tag{4}$$

$$\text{GDOP} = \sqrt{D_{11} + D_{22} + D_{33} + D_{44}} \tag{5}$$

$$\text{HDOP} = \sqrt{D_{11} + D_{22}}. \tag{6}$$

E. Method for Calculating the SVDOP

Fig. 15 illustrates the relationship between the spherical coordinate system and the Cartesian coordinate system.

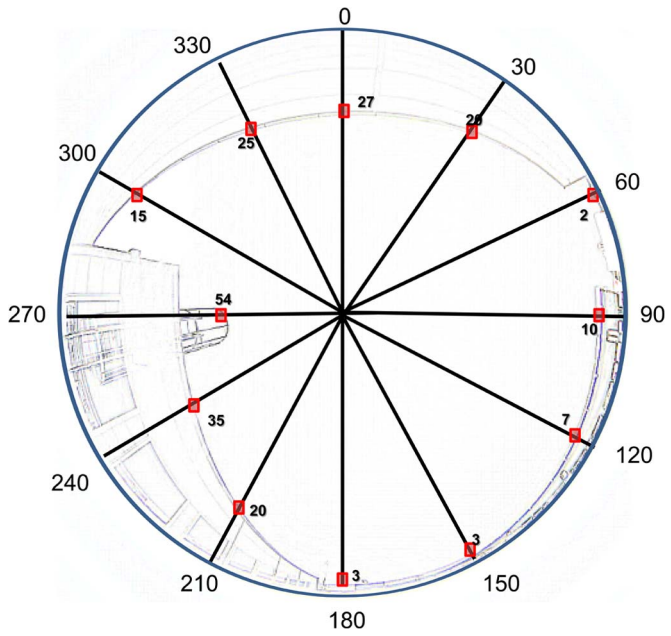

Fig. 16. Azimuth and elevation angle.

The coordinates of a sky-view singularity point i observed through a fish-eye lens can be expressed by the azimuth Φ_i and the elevation angle θ_i of the spherical coordinate system, and these can be converted to x_i, y_i, z_i in the Cartesian coordinate system. The azimuth and the elevation angle are shown in Fig. 16. The conversion formula from the spherical coordinate system to the Cartesian coordinate system is given in

$$\begin{aligned} x_i &= r\cos(\theta_i)\cos(\phi_i) \\ y_i &= r\cos(\theta_i)\sin(\phi_i) \\ z_i &= r\sin(\theta_i) \end{aligned} \tag{7}$$

where r is the distance of the singularity point that is projected onto the spherical coordinate system from the center of the fish-eye lens, and all the rs of the sky-view singularity points are the same. When the ith row of the h_i of the matrix H in (3) is applied to the coordinates of a virtual navigation satellite acquired from the sky view, the following can be derived:

$$h_i = \begin{bmatrix} -\cos(\theta_i)\cos(\phi_i) \\ -\cos(\theta_i)\sin(\phi_i) \\ -\sin(\theta_i) \end{bmatrix}^T. \tag{8}$$

When (8) is applied to each of the singularity points in order to calculate H and is used to calculate the DOP, the result is the SVDOP.

F. Calculation of SVDOP Using Singularity Points

The SVF is 0.5 in the case in which the periphery is blocked off in a circular fashion, as in Fig. 17, and in the case where the lower semicircle is blocked off, as in Fig. 18. Both cases are the virtual environments of SVF 0.5.

Equation (8) is used to apply the singularity points of an actual sky-view image in order to calculate H, which is then utilized to calculate the DOP. When the periphery is blocked off in a circular fashion, as shown in Fig. 17, the SVDOP is calculated as 0.66, and when the lower semicircle is blocked off, as shown in Fig. 18, the SVDOP is calculated as 0.91.

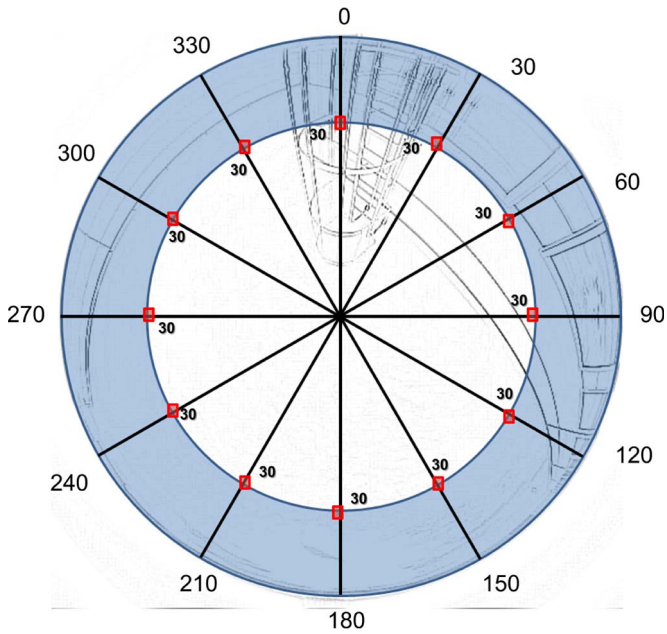

Fig. 17. Virtual Environment 1 of SVF 0.5.

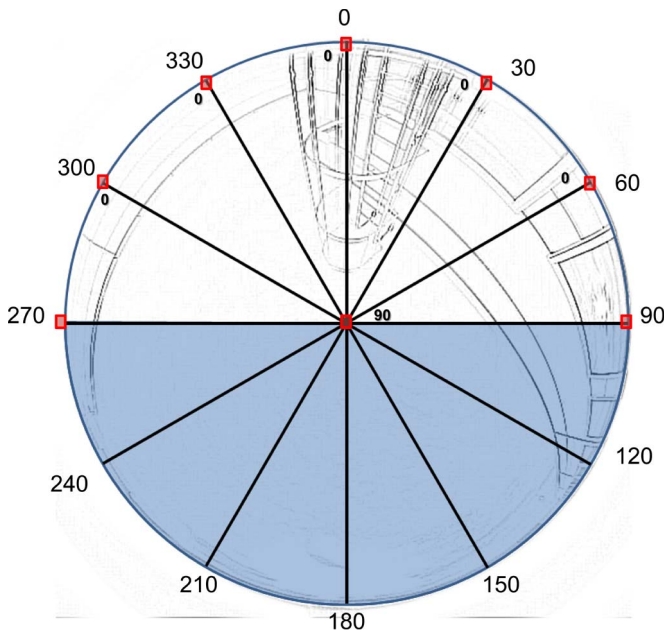

Fig. 18. Virtual Environment 2 of SVF 0.5.

G. Calculation of SVDOP Using Actual Singularity Point Measurement

Figs. 19 and 20 show the singularity points of configurations 1 and 2.

Equation (8) is used to apply the singularity points of an actual sky-view image in order to calculate H, which is then utilized to calculate the DOP. When the actual SVDOP was calculated, it was confirmed to be 0.64 and 0.70 for station 1 and station 2, respectively.

H. Comparison the DOP and SVDOP

When the sky view of the two stations is to be observed, the SVF is 0.31, but the DOP is different, as shown in Table I. Figs. 21 and 22 show the calculated DOP using real data.

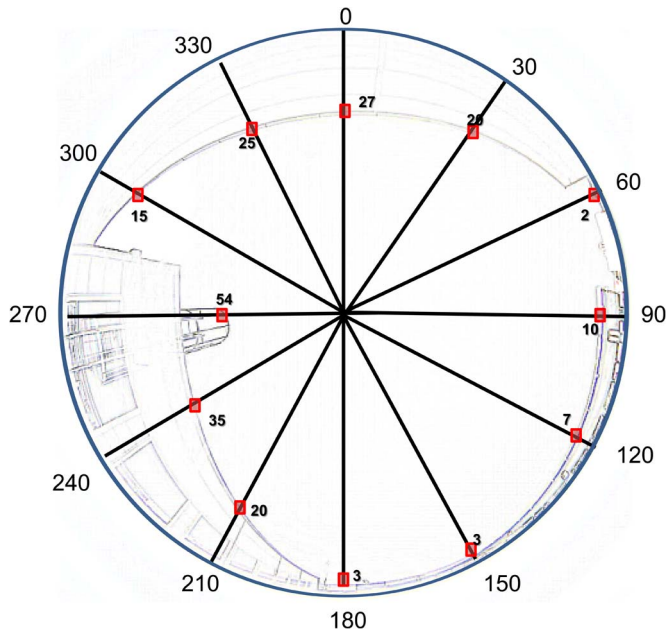

Fig. 19. Azimuth and elevation angle of station 1.

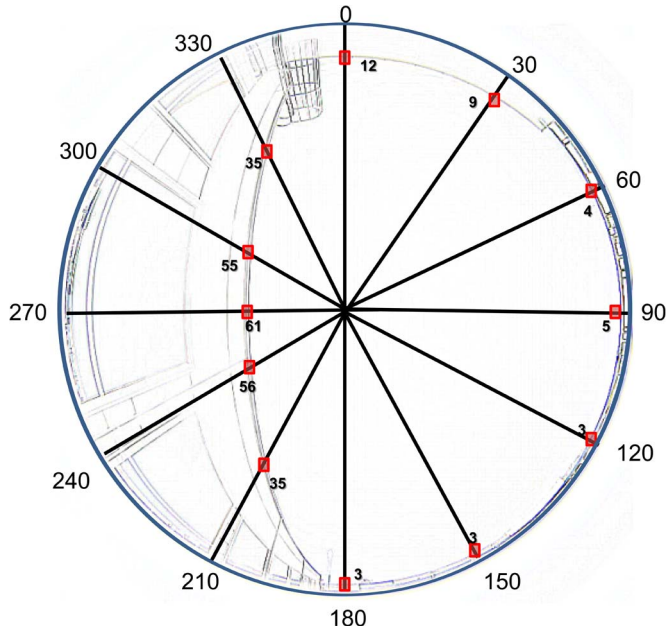

Fig. 20. Azimuth and elevation angle of station 2.

TABLE I
COMPARISON OF THE SVF, THE GDOP, AND THE SVDOP

	SVF	GDOP (AVERAGE)	SVDOP
Station 1	0.31	1.85	0.64
Station 2	0.31	2.43	0.70
Virtual Station1	0.5	-	0.66
Virtual Station2	0.5	-	0.91

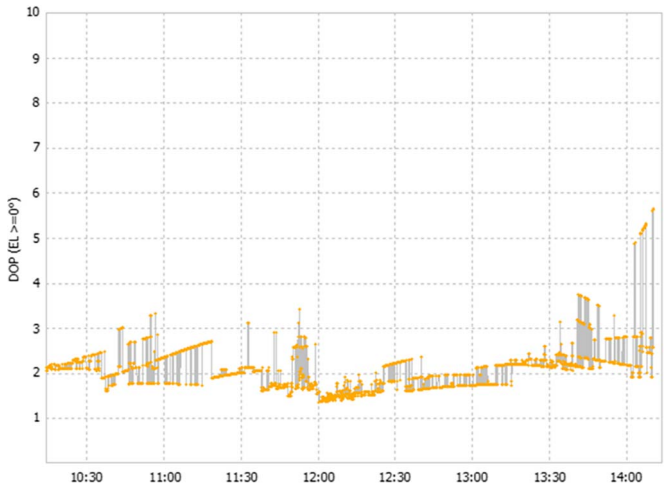

Fig. 21. GDOP of configuration 1.

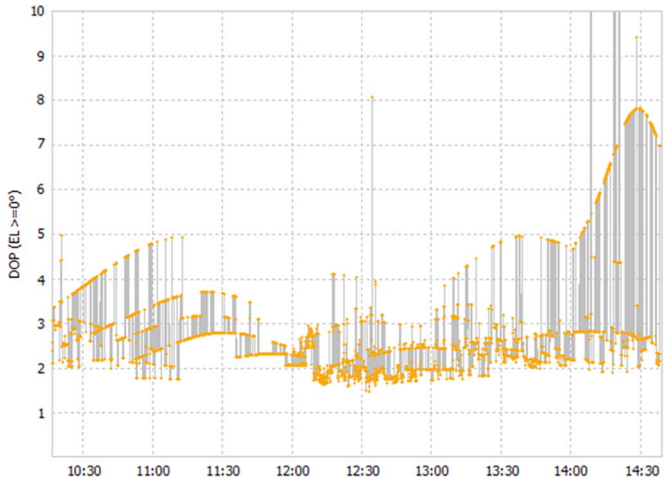

Fig. 22. GDOP of configuration 2.

V. Conclusion

This paper has proposed the SVDOP as a performance index that is highly useful when positioning is carried out using GNSS signals in a land transportation environment. In this paper, it was confirmed through experiments that when the conventional SVF is used in a land transportation environment, the predicted value for the positioning performance using the GNSS is often not consistent with the actual positioning error. When the SVDOP was applied, however, the predicted value proved to be substantially close to the actual positioning error. There is a need for future research, however, to confirm the results of the SVDOP using the proposed method in actual land transportation environments. In this paper, the SVDOP was calculated with real Global Positioning System data, and the usefulness of the SVDOP was validated by comparing it with the conventional SVF and the DOP.

References

[1] L. Chapman, "Short communication sky-view factor approximation using GPS receivers," *Int. J. Climatol.*, vol. 22, pp. 615–621, 2002.
[2] M. J. Brown, "Comparison of methodologies for computing sky view factor in urban environment," Los Alamos Natl. Lab., Los Alamos, NM, USA, Internal Rep. LA-UR-01-4107, 2001.
[3] K. Blennow, "Sky view factors from high resolution scanned fish-eye lens photographic negatives," *J. Atmos. Ocean. Technol.*, vol. 12, no. 6, pp. 1357–1362, Dec. 1995.
[4] A. N. Matori, "Quality assessment of DTM generated from RTK GPS data on area with various sky view," in *Proc. ION GNSS*, Sep. 16–19, 2008, pp. 1462–1469.
[5] C. S. B. Grimmond, "Rapid methods to estimate sky-view factors applied to urban areas," *Int. J. Climatol.*, vol. 21, no. 7, pp. 903–913, Jun. 2001.
[6] D. G. Steyn, "The determination of sky view factors in urban environments using video imagery," *J. Atmos. Ocean. Technol.*, vol. 3, no. 4, pp. 759–764, Dec. 1986.
[7] T. Gal, "Comparison between sky view factor values computed by two different methods in an urban environment," *Acta Climatol. Chorologica*, vol. 40, no. 41, pp. 17–26, 2007.
[8] L. Chapman, "Improved one dimensional energy balance modeling utilizing sky-view factors determined from digital imagery," presented at the Proc. 10th SIRWEC Conf., Davos, Switzerland, Mar. 22–24, 2000.
[9] W. Hong, "New indicator of signal blocking degree to describe GNSS signal receiving environment in land road," in *Proc. ION PNT*, 2013, pp. 192–197.
[10] L. Chapman, "Real-time sky-view factor calculation and approximation," *J. Atmos. Ocean. Technol.*, vol. 21, no. 5, pp. 730–741, May 2003.
[11] A. Leick, *GPS Satellite Surveying*. Hoboken, NJ, USA: Wiley, 2003.
[12] B. Hofmann-Wellenhof, H. Lichtenegger, and E. Wasle, *GNSS Global Navigation Satellite System: GPS, GLONASS, Galileo and More*. New York, NY, USA: Springer-Verlag, 2007.

Stochastic Park-and-Charge Balancing for Fully Electric and Plug-in Hybrid Vehicles

Florian Häusler, Emanuele Crisostomi, Arieh Schlote, Ilja Radusch, and Robert Shorten

***Abstract*—Motivated by the need to provide services to alleviate range anxiety of electric vehicles, we consider the problem of balancing charging demand across a network of charging stations. Our objective is to reduce the potential for excessively long queues to build up at some charging stations, although other charging stations are underutilized. A stochastic balancing algorithm is presented to achieve these goals. A further feature of this algorithm is that it is fully decentralized and facilitates a plug-and-play type of behavior. Using our system, the charging stations can join and leave the network without any changes to, or communication with, a centralized infrastructure. Analysis and simulations are presented to illustrate the efficacy of our algorithm.**

***Index Terms*—C2X, charging stations, electric vehicles (EVs), parking, plug-in hybrid vehicle, simulation, stochastic balancing.**

Manuscript received May 9, 2013; revised August 1, 2013 and September 23, 2013; accepted October 2, 2013. Date of publication November 1, 2013; date of current version March 28, 2014. This work was supported in part by the Science Foundation Ireland under Grant 11/PI/1177 and in part by the European Commission's Seventh Framework Programme FP7-ICT through TEAM. The Associate Editor for this paper was L. Li.

F. Häusler and I. Radusch are with Fraunhofer Institute for Open Communication Systems (FOKUS), 10589 Berlin, Germany.
E. Crisostomi is with the Department of Energy, Systems, Territory, and Construction Engineering, University of Pisa, 56126 Pisa, Italy.
A. Schlote is with National University of Ireland, Maynooth (NUIM), Maynooth, Ireland.
R. Shorten is with IBM Research-Ireland, Dublin, Ireland.

Color versions of one or more of the figures in this paper are available online at http://ieeexplore.ieee.org.
Digital Object Identifier 10.1109/TITS.2013.2286266